

Original Article

MiR-374b-5p inhibits KDM5B-induced epithelial-mesenchymal transition in pancreatic cancer

Xin Zhao*, Xiaoshi Zhang*, Xinxue Zhang, Tao Jiang, Jialei Zhai, Huaguang Wang, Mengxiu Huang, Ren Lang, Qiang He

Department of Hepatobiliary Surgery, Beijing Chao-Yang Hospital, Affiliated to Capital Medical University, Beijing, China. *Equal contributors.

Received September 9, 2020; Accepted June 18, 2021; Epub August 15, 2021; Published August 30, 2021

Abstract: Micro(mi)RNAs play a critical regulatory role in the progression and metastasis of pancreatic cancer (PC). In this study, we aimed to reveal the mechanisms of miR-374b-5p in regulating epithelial-mesenchymal transition (EMT) in PC. Gene Expression Omnibus datasets (GSE24279 and GSE71533) and the pancreatic ductal adenocarcinoma (PDAC) cohort of The Cancer Genome Atlas were employed to screen for potential prognostic miRNAs. The expression of miR-374b-5p was measured by quantitative real-time polymerase chain reaction (qRT-PCR) in 78 paired PDAC tissue samples. The biological effects of miR-374b-5p were investigated using *in vitro* and *in vivo* assays. Luciferase reporter assays and immunohistochemical tests were conducted to verify the interaction between miR-374b-5p and its predicted direct target, KDM5B. MiR-374b-5p was downregulated in PC tissues, and a low level of miR-374b-5p was associated with poor overall survival, greater tumor size, and more lymph node metastasis in PC. *In vitro* assays indicated that overexpression of miR-374b-5p suppressed the proliferation, migration, and invasion of PC cells. Mechanistically, miR-374b-5p suppressed the expression of KDM5B, which inhibited E-cadherin expression but promoted N-cadherin and vimentin expression. Finally, *in vivo* assays demonstrated that miR-374b-5p overexpression suppressed tumor growth and lung metastasis in PANC-1 cells. Thus, our findings indicate that miR-374b-5p could be a potential prognostic biomarker and therapeutic target for KDM5B-induced EMT in PC.

Keywords: miR-374b-5p, KDM5B, epithelial-mesenchymal transition, pancreatic cancer

Introduction

Pancreatic cancer (PC), a lethal cancer, has a dismal five-year overall survival (OS), with a range of 5-9% [1-4]. Its most common pathological type is pancreatic ductal adenocarcinoma (PDAC), which accounts for over 90% of all PC cases [5]. PDAC is not sensitive to most chemotherapeutic and molecular targeted agents. Consequently, radical resection remains the most effective treatment for achieving long-term survival in PC [6]. However, because of aggressive invasion and metastasis, most patients are not diagnosed with PC until it has reached an advanced stage and thus miss the opportunity to undergo curative surgery [7].

Epithelial-mesenchymal transition (EMT) is a critical event that occurs during cancer development. During EMT, mesenchymal markers,

such as N-cadherin and vimentin, are activated, facilitating cell metastasis [8]. Therefore, understanding the molecular modulation mechanisms underlying EMT is vital to identify potential biomarkers and therapeutic targets for PC.

Micro(mi)RNA, a noncoding small molecule RNA, generally degrades the target mRNAs by binding to the 3'-untranslated region (3'-UTR) [9]. Evidence indicates that miRNAs play a critical regulatory role in PC progression. For example, miR-21 and miR-203 are overexpressed in tumor tissues and negatively correlated with the OS of patients with PC [10, 11]. Additionally, miR-145 and miR-122-5p, which inhibit EMT by targeting TGF- β and CCNG1, were downregulated in PC tissues [12, 13]. Furthermore, many studies have demonstrated that miRNAs regulate tumorigenesis by interacting with other noncoding RNAs [14]. For instance, by sponging

miR-217, circular RNA ADAM9 increases PRSS3 expression and thus activates the ERK/VEGF signaling pathway in PC [15]. Long noncoding RNA HCP5 can sponge miR-214-3p and repress its suppressive function on HDGF, leading to gemcitabine resistance in PC [16]. In such interactions, termed competing endogenous RNA networks, the miRNAs act as a bridge between the noncoding RNAs and the mRNAs to regulate tumor progression. Thus, identifying EMT-associated miRNAs can improve the search for novel therapeutic PC targets.

In this study, we used public miRNA expression profiles to identify miR-374b-5p as a prognostic biomarker for PC. We further investigated its effects on EMT in PC and the underlying mechanisms.

Materials and methods

Screening overall survival-associated and differentially expressed (DE) microRNAs in pancreatic cancer

Two miRNA expression profiles, GSE24279 and GSE71533, were downloaded from the Gene Expression Omnibus (GEO) database (<https://www.ncbi.nlm.nih.gov/geo/>). We performed differential expression analyses with the “limma” R package and set the selection criterion as $P < 0.05$ to identify the intersected DE miRNAs. Next, the miRNA expression dataset and clinical data of the PDAC cohort were extracted from The Cancer Genome Atlas (TCGA) database (<https://gdac.broadinstitute.org/>). In this cohort, we excluded cases wherein the patients died within three months of operation, since these deaths were mainly attributed to surgical complications, and this factor could have interfered with the evaluation of long-term survival. Based on the median expression value of the DE miRNAs, the patients with PC were then classified into high- and low-expression level groups to perform Kaplan-Meier (K-M) survival analyses. Finally, we identified potential DE miRNAs associated with the OS of the PDAC cohort.

Functional analyses and target prediction for miR-374b-5p

We applied the DIANA-mirPath web tool to discover the underlying pathways associated with miR-374b-5p. Using the miRWalk 2.0 web tool, a putative target gene set of miR-374b-5p was

predicted. Then, we performed Pearson’s correlation analyses to screen out a negatively associated gene set corresponding to miR-374b-5p, using the mRNA and miRNA expression profiles of the PDAC cohort of TCGA. These two gene sets were then intersected to obtain the target genes of miR-374b-5p. Next, Gene Ontology (GO) annotation and Kyoto Encyclopedia of Gene and Genomes (KEGG) pathway enrichment analysis were conducted to uncover the potential functions of the target genes of miR-374b-5p, using the “clusterProfiler” R package.

Patients and samples in the validation cohort

From January 2019 to May 2020, 78 patients with PC in Beijing Chao-Yang Hospital were enrolled in the validation cohort. The patients were diagnosed with PDAC based on histopathological evidence. Adjuvant radiotherapy and chemotherapy were not performed preoperatively. Paired tumor and adjacent healthy tissues were immediately frozen in liquid nitrogen for 2 h and stored at -80°C . Quantitative real-time polymerase chain reaction (qRT-PCR) was performed to determine the miR-374b-5p level. We plotted a receiver operating characteristic (ROC) curve and calculated the area under the curve (AUC) to evaluate the significance of miR-374b-5p in distinguishing tumor tissues from normal tissues. The patients were classified into high- and low-level groups according to the median expression value of miR-374b-5p. Then, we compared the clinicopathological variables between the two groups. This study was permitted by the research ethics committee of Chao-Yang hospital, and all patients signed an informed consent form (No. 2019-S-243).

Quantitative real-time polymerase chain reaction

Total RNA from cell and tissue samples was extracted using TRIzol reagent (Invitrogen, CA, USA) and transcribed into the first-strand cDNA using rtStar™ First-Strand cDNA Synthesis Kit (Arraystar Inc., Rockville, MD, USA) following the manufacturer’s protocol. The primers were designed and synthesized by Yingjun Biotechnology Co., Ltd. (Shanghai, China). The sequences of the forward and reverse primers for miR-374b-5p were 5'-ACACTCCAGCTGGGATATAACAACCTGC-3' and 5'-CTCAACTGGTGTTCGTGGAGTCGGCAATTCAGTGTGAGCACTTAGC-3', respectively. Following the

miR-374b-5p inhibits EMT in pancreatic cancer

manufacturer's instructions, qRT-PCR was performed with Arraystar SYBR® Green Real-time qPCR Master Mix (Arraystar Inc.). Relative RNA expression was calculated using the $2^{-\Delta\Delta CT}$ method and normalized to the expression level of β -actin.

Cell culture and transfection

Human pancreatic cancer cells (PANC-1, AsPC-1, MIA PaCa-2, and SW1990) and normal pancreatic ductal cells (HPDE6-C7) were purchased from the American Type Culture Collection (Manassas, VA, USA) and cultured with Dulbecco's modified Eagle's medium (DMEM) supplemented with 10% fetal bovine serum (TransGen Biotech, Beijing, China). The cells were grown as monolayers in a humidified CO₂ incubator at 37°C.

Human miR-374b-5p negative control (NC), mimics, and inhibitor were purchased from RiboBio Co., Ltd. (Guangzhou, China). Short hairpin (sh)-RNA vector for Lysine Demethylase 5B (KDM5B) and KDM5B pcDNA3.1 expression vector were purchased from GenePharma Co., Ltd. (Suzhou, China) to change the expression level of KDM5B in PC cells. PANC-1 and SW1990 cells were seeded into 6-well plates, and transfection was performed using Lipofectamine 3000 (Invitrogen) according to the manufacturer's instructions. GV248 lentiviral vectors carrying miR-374b-5p mimics and NC were constructed by GeneChem Co., Ltd. (Shanghai, China) in HEK 293T cells. PANC-1 cells were transfected with lentiviral vectors, and stable miR-374b-5p-overexpressing cells were selected with puromycin for 14 days.

Cell counting kit-8 (CCK-8) assay

PANC-1 and SW1990 cells were transfected for 24 h and seeded into 96-well plates at a density of 3×10^3 cells/well with 100 μ L of complete medium at 37°C. Cells were incubated for 0, 24, 48, 72, and 96 h, and a CCK-8 assay (Yuan Yuan Biotech Inc., Guangzhou, China) was performed following the manufacturer's protocol to measure cell proliferation. Optical densities were examined at 450 nm. All experiments were performed in triplicate.

Cell migration assay

Transwell chambers (Corning 3422, NY, USA) were used to detect the migration abilities of

PANC-1 and SW1990 cells. The lower chamber was filled with 100 μ L DMEM with high glucose. Then, 24 h after transfection, 5×10^4 cells in 100 μ L of serum-free DMEM were seeded into the upper chamber. After 24 h of incubation, the migrated cells were fixed with 4% paraformaldehyde for 15 min and stained with 0.1% crystal violet (Beyotime, Shanghai, China) for 15 min. The stained cells were then photographed at 200 \times magnification and counted in five fields using a light microscope (Olympus, Tokyo, Japan).

Cell scratch wound assay

After 24 h of transfection, 5×10^7 PC cells/well were seeded into a 12-well plate. Again, after 24 h of incubation, wounds were created using a 200 μ L pipette tip, and the cells were washed twice with phosphate-buffered saline (PBS). Images were captured after 0, 24, and 48 h, and wound width was subsequently measured in triplicate for each group.

Western blot (WB) analysis

Antibodies for KDM5B, E-cadherin, N-cadherin, vimentin, and GAPDH were purchased from Abcam (Shanghai, China). Briefly, PANC-1 and SW1990 cells were seeded into 6-well plates at a concentration of 5×10^5 cells/mL. After 24 h of transfection, PC cells were collected using a scraper and lysed using RIPA lysis buffer (Beyotime). Total protein concentration was measured using the BCA Protein Assay Kit (Beyotime) following the manufacturer's instructions. NuPAGE™ LDS Sample Buffer 1 \times (Thermo Scientific, CA, USA) was added to the protein samples and boiled for 10 min. Next, the proteins were separated on precast NuPAGE™ 4-12% Bis-Tris Midi Protein Gels (Thermo Scientific) and electrotransferred onto polyvinylidene fluoride membranes. The bound antibodies were visualized using BeyoECL Plus (Beyotime) and WB detection instruments (Clinx Science, Shanghai, China).

Luciferase reporter assay

The wild-type (WT) and mutant (MUT) 3'-UTR fragments of KDM5B containing miR-374b-5p binding sites were cloned and inserted into the primir-RB-Report™ vector (RiboBio). HEK 293T cells were co-transfected with 50 nM miR-374b-5p mimics and 500 ng/mL plasmid. After 48 h, the luciferase activity of each group

was measured using the Dual-Luciferase Reporter Assay System (Promega, Madison, WI, USA), following the manufacturer's instructions. All assays were performed in triplicate.

Xenograft tumor model and metastasis assays

miR-374b-5p-overexpressing and NC lentiviruses were constructed and purchased from GenePharma Co., Ltd. Ten male BALB/c nude mice (6 weeks old) were purchased from SLAC Laboratory Animal Center, Shanghai, China, and were randomly categorized into two groups of five. Briefly, 4×10^6 PANC-1 cells, transfected with miR-374b-5p lentivirus or NC lentivirus (200 μ L DMEM), were subcutaneously injected into the right posterior back region of the mice. Tumor volume was calculated using the following formula: tumor volume = $0.5 \times \text{length} \times \text{width}^2$. After 18 days, the tumors were excised and weighed. For the *in vivo* metastasis assays, ten male BALB/c nude mice (6 weeks old) were randomly assigned to two groups. In each group, 1×10^6 PANC-1 cells (100 μ L DMEM) stably expressing miR-374b-5p or NC were injected into the tail vein of the nude mice. Four weeks later, the mice were sacrificed, and their lungs were harvested for hematoxylin-eosin (HE) staining and metastatic foci counting. All animal experiments were approved by the Animal Care and Use Committee of Beijing Chao-Yang Hospital, and all possible measures were undertaken to minimize animal suffering.

Immunohistochemistry analyses

To evaluate the protein expression level of KDM5B, we chose ten paired PDAC samples and performed immunohistochemistry (IHC) assays. Briefly, paraffin-embedded tissue specimens were sectioned and incubated with anti-KDM5B primary antibody (1:200; ZSGB-BIO, Beijing, China) overnight at 4°C. After washing with PBS, HRP-conjugated secondary antibody (goat anti-rabbit IgG; BOSTER, Hangzhou, China) was added to the slides for 1 h of incubation. 3,3'-Diaminobenzidine (DAB) substrate solution was the chromogen used for KDM5B visualization. The intensity of KDM5B cytoplasmic staining was graded as 0 (negative), 1+ (weak), 2+ (moderate), or 3+ (strong). The H-score ($1 \times [\% \text{ cells } 1+] + 2 \times [\% \text{ cells } 2+] + 3 \times [\% \text{ cells } 3+]$) was used to reflect KDM5B staining.

Statistical analysis

R software version 3.6.0 was used to integrate and analyze the data. Raw miRNA and mRNA expression data were normalized and \log_2 -transformed. We determined the significant differences between groups and produced figures using GraphPad Prism 8 (v8.0.2.263, GraphPad, Inc., CA, USA). Pearson's correlation analysis was used to identify the relationship between miR-374b-5p level and mRNA expression values. A paired-sample *t*-test or two-sample variance was used to compare the continuous variables. The Wilcoxon signed-rank test was utilized to analyze the correlation between the miR-374b-5p level and clinicopathological parameters. Fisher's exact test was used to compare the categorical variables among the groups. $P < 0.05$ was considered significant.

Results

The low miR-374b-5p level was associated with the poor prognosis of pancreatic cancer

In the GSE24279 and GSE71533 datasets, we found 126 DE miRNAs, of which 18 were significantly associated with the clinical outcomes of the PDAC cohort from TCGA (**Figure 1A**). Of these 18 miRNAs, 12 showed consistent variation in the PC tumor tissues of the two GEO datasets. The expression levels of six DE miRNAs were reasonably associated with the OS of PC patients, thereby implying that upregulated miRNAs in PC tumors were related to poor OS, and downregulated miRNAs were correlated with favorable prognosis (**Figure 1B**). Among the six miRNAs, miR-374b-5p exhibited a decreased level in the PC tumors and was significantly associated with a good prognosis in patients with PC (**Figure 1C-E**). Therefore, we selected miR-374b-5p to analyze potential functions and target genes affecting PC progression.

We assessed the expression of miR-374b-5p in 78 patients with PDAC using qRT-PCR and observed that its expression was significantly downregulated in the tumor samples compared to that in the normal samples (**Figure 1F**). ROC curve analysis showed that miR-374b-5p was a significant factor in distinguishing tumor samples from normal samples (AUC = 0.846, **Figure 1G**). Next, we categorized all 78 patients into high- and low-level groups according to the

miR-374b-5p inhibits EMT in pancreatic cancer

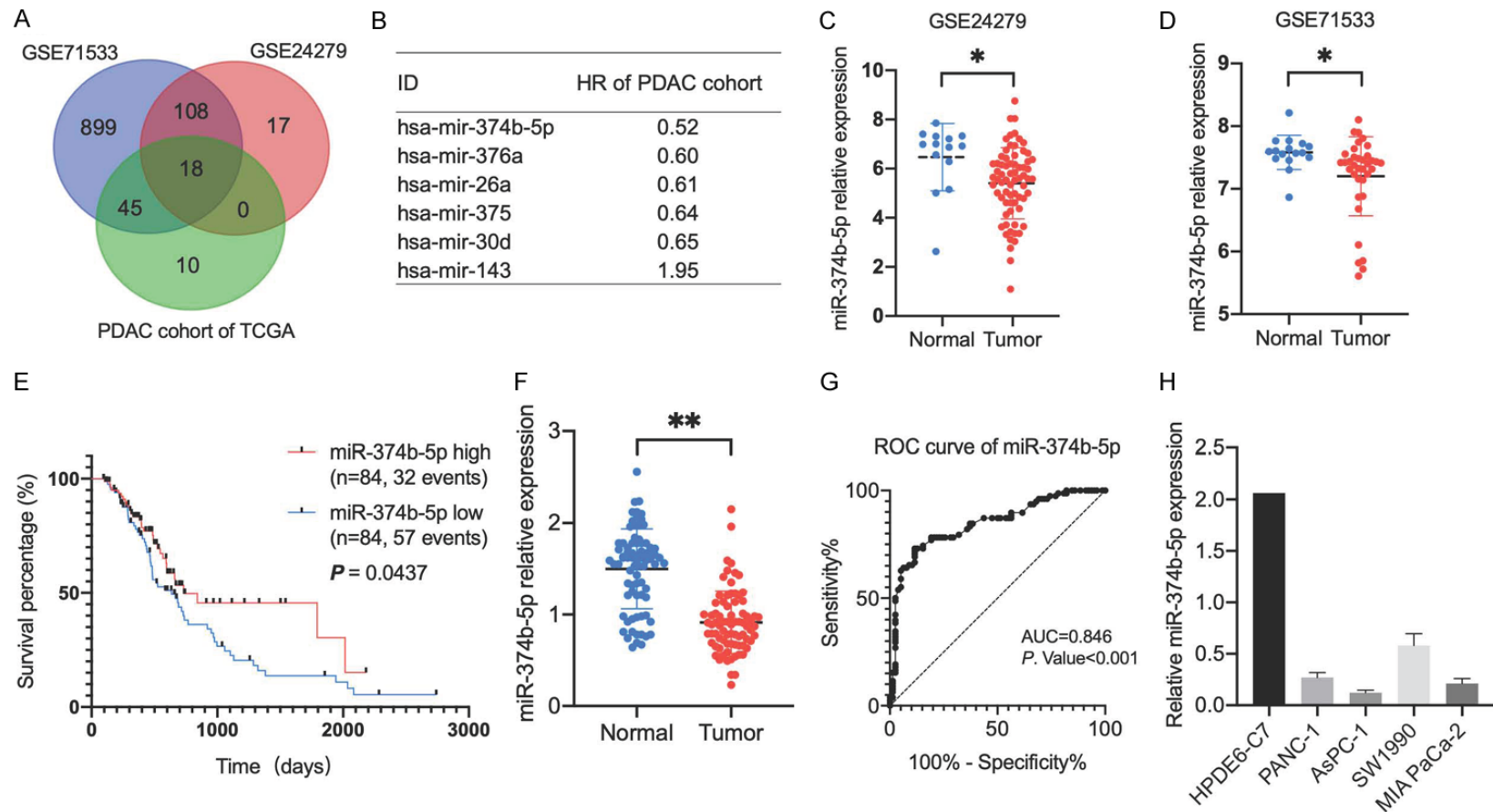


Figure 1. MiR-374b-5p was downregulated in PC. A. Venn diagram identifying 18 clinically significant miRNAs that were differentially expressed in the GSE71533 and GSE24279 datasets and were associated with prognosis in the PDAC cohort of TCGA. B. Hazard ratio of six miRNAs based on K-M survival analysis of the TCGA PDAC cohort. C and D. Expression of miR-374b-5p in the GSE24279 and GSE71533 datasets. E. K-M survival analysis of miR-374b-5p in the TCGA PDAC cohort. F. Expression of miR-374b-5p in 78 paired PC tissues measured by qRT-PCR. G. Receiver operating characteristic curve analysis revealed that miR-374b-5p could be used to distinguish PC samples from normal samples. H. Expression of miR-374b-5p in PC cells and normal pancreatic ductal cells. * $P < 0.05$; ** $P < 0.01$. PC, pancreatic cancer; PDAC, pancreatic ductal adenocarcinoma; TCGA, The Cancer Genome Atlas; K-M, Kaplan-Meier; qRT-PCR, quantitative real-time polymerase chain reaction.

miR-374b-5p inhibits EMT in pancreatic cancer

Table 1. Association between miR-374b-5p level and clinico-pathological parameters of patients with pancreatic ductal adenocarcinoma in the study cohort

Clinical parameters	miR-374b-5p		P value
	Low (n = 39)	High (n = 39)	
Age (years)	62.2 ± 10.9	60.8 ± 11.3	0.281
Gender			
Male	22	18	0.497
Female	17	21	
Pathological differentiation			0.451
Moderate and high	26	30	
Poor	13	9	
Tumor size (cm)	4.4 ± 2.5	3.0 ± 1.7	< 0.001
Resection			
R0	29	33	0.400
R1 and R2	10	6	
Numbers of positive lymph node	4.1 ± 4.4	2.4 ± 2.8	0.026
Vascular invasion			
Negative	27	26	1.000
Positive	12	13	
TNM stage			0.610
I-III	9	12	
IV-VI	30	27	
Primary tumor			0.022
T1 and T2	23	33	
T3 and T4	16	6	
Reginal lymph nodes			0.620
N0	10	13	
N1 and N2	29	26	
Distant metastases			0.711
Negative	34	36	
Positive	5	3	

Tumor-node-metastasis (TNM) stage was based on the 8th edition of the American Joint Committee on Cancer.

median value of the miR-374b-5p expression. The univariate analysis results indicated that the tumor size, the number of positive lymph nodes, and ratio of T3 and T4 were significantly increased in the low-level group compared to those in the high-level group (**Table 1**).

We also examined the expression level of miR-374b-5p in several pancreatic cell lines and observed that the level was relatively more upregulated in normal pancreatic ductal cells (HPDE6-C7) than in PC cells (PANC-1, AsPC-1, SW1990, and MIA PaCa-2; **Figure 1H**). These results indicated that the downregulation of miR-374b-5p was associated with the malignant phenotype of PC.

miR-374b-5p inhibited the proliferation and migration ability of pancreatic cancer cells

To investigate the role of miR-374b-5p in regulating the progression of PC cells, we altered miR-374b-5p expression using mimics and inhibitors. In PANC-1 and SW1990 cells, the CCK-8 assays showed that miR-374b-5p overexpression and inhibition significantly suppressed and promoted cell proliferation, respectively (**Figure 2A**). In the transwell migration assays, miR-374b-5p expression significantly reduced the migration abilities of PANC-1 and SW1990 cells (**Figure 2B**). The scratch wound assays also indicated that miR-374b-5p served as an inhibitor of PC cell migration (**Figure 2C**). Collectively, these assays demonstrated that miR-374b-5p suppressed the proliferation and migration abilities of PC cells.

miR-374b-5p may be involved in cancer-associated pathways

To further understand the relationship between miR-374b-5p and PC progression, we performed pathway enrichment analyses with DIANA-mirPath. MiR-374b-5p was enriched in multiple cancer-associated pathways, including p53 signaling, FoxO

signaling, and proteoglycans of cancer (**Figure 3A**). Using miRWalk 2.0, we predicted 2292 genes with a miRNA response element in their 3'-UTRs by mapping them to miR-374b-5p. In this gene set, 135 genes showed a negative correlation with miR-374b-5p, according to the PDAC cohort of TCGA. Thus, we chose these 135 genes as the target genes of miR-374b-5p to perform further functional analyses (**Figure 3B**).

GO annotation of miR-374b-5p target genes suggested that "positive regulation of cellular protein localization" was the most enriched term in the biological process category (**Figure 3C**). "Coated membrane" and "adherens junctions" were the most enriched terms in the cellular component category.

miR-374b-5p inhibits EMT in pancreatic cancer

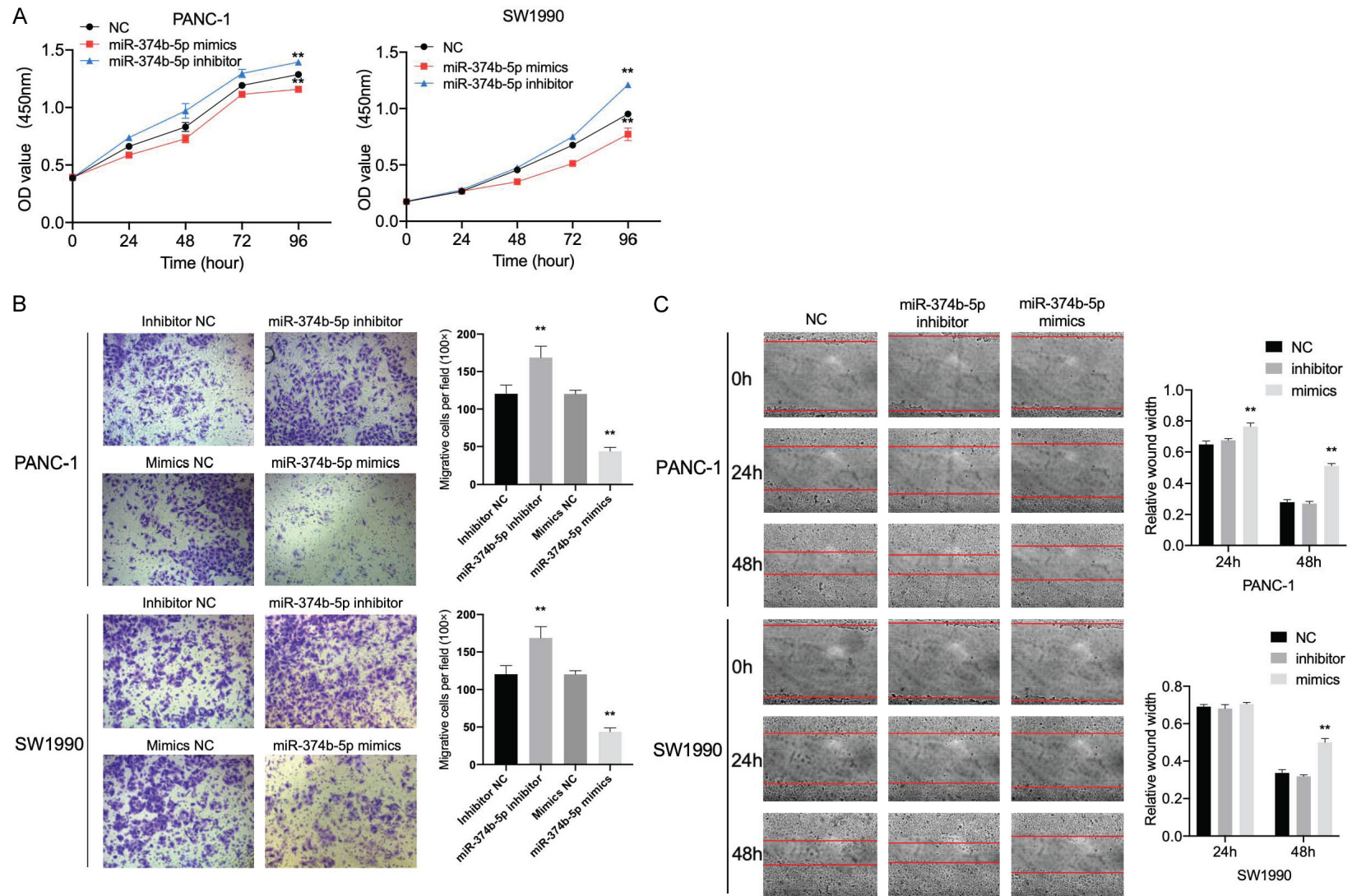


Figure 2. MiR-374b-5p inhibited the proliferation and migration of pancreatic cancer cells. A. Cell counting kit-8 assays. B. Transwell migration assays. C. Cell scratch wound assays. $**P < 0.01$ vs. the NC group. NC, negative control.

miR-374b-5p inhibits EMT in pancreatic cancer

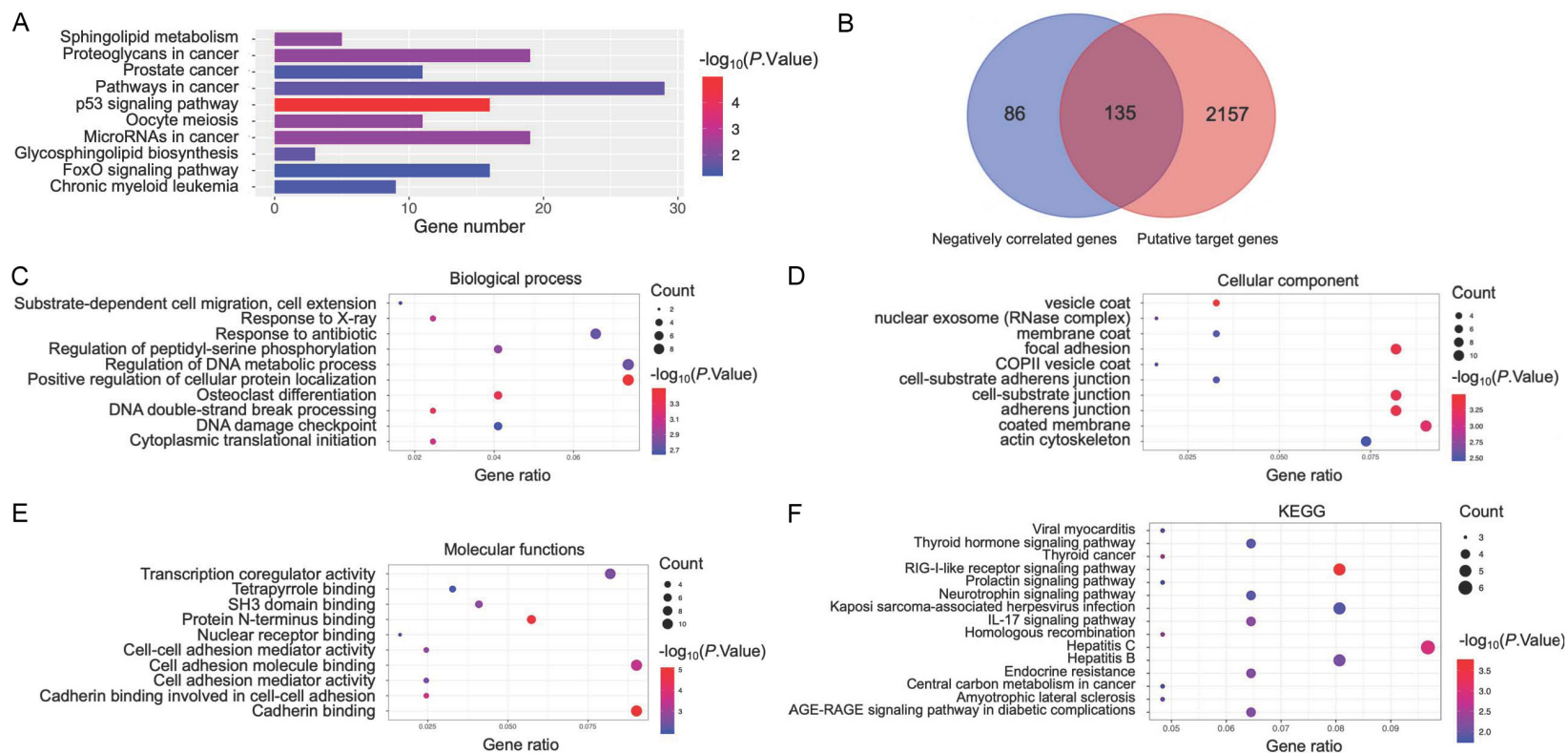


Figure 3. MiR-374b-5p was found to be involved in cancer-associated pathways. A. The results obtained using the DIANA-mirPath tool indicate that miR-374b-5p plays a critical role in tumor-associated signaling pathways. B. According to the miRWalk database, there were 135 putative target genes of miR-374b-5p, which were negatively correlated with the miR-374b-5p level. C-E. Gene Ontology analysis of miR-374b-5p target genes. F. Kyoto Encyclopedia of Gene and Genomes pathway enrichment analysis of the miR-374b-5p target genes.

tion” were the most enriched terms in the cellular component category (**Figure 3D**), and most genes of the molecular function category were enriched in “cell adhesion molecule binding” and “cadherin binding” (**Figure 3E**). In the KEGG pathway analyses, six genes were associated with virus infections such as hepatitis C and herpesvirus (**Figure 3F**). Collectively, the results of the bioinformatics analyses indicated that miR-374b-5p function was associated with tumor progression. Notably, the miR-374b-5p level was negatively associated with the increase in the number of metastatic lymph nodes (**Table 1**), and its target genes were associated with adherens junction, cell-substrate junction, actin cytoskeleton, focal adhesion, and cadherin binding in the GO analyses. These findings suggest that miR-374b-5p probably regulates the EMT process, which is a prominent phenotype of tumor invasion and is characterized by dysfunctions of the cell junction.

miR-374b-5p targets Lysine Demethylase 5B (KDM5B) in pancreatic cancer

Based on the TargetScan database, two binding sites of miR-374b-5p matched with the 3'-UTR of KDM5B (**Figure 4A**). In the PDAC cohort of TCGA, the expression of KDM5B was negatively correlated with the level of miR-374b-5p (**Figure 4B**). Luciferase reporter assays showed that miR-374b-5p mimics markedly decreased the relative luciferase activity of KDM5B-WT in HEK 293T cells. However, the luciferase activity of KDM5B-MUT was not affected by the miR-374b-5p mimics (**Figure 4C**). In the WB analyses, KDM5B expression was significantly suppressed in the PANC-1 and SW1990 cells transfected with miR-374b-5p mimics. In contrast, the KDM5B level was increased in the PC cells transfected with the miR-374b-5p inhibitor (**Figure 4D**). These observations indicated that KDM5B could be a direct target of miR-374b-5p.

KDM5B promoted the epithelial-mesenchymal transition process in pancreatic cancer cells

To investigate the effect of KDM5B on EMT, we transfected lentiviral vectors encoding KDM5B (overexpression group, OE) and sh-KDM5B (knockdown group, KD) into PANC-1 and SW1990 cells. As shown in **Figure 4E**, KDM5B-OE promoted the expression of

N-cadherin and vimentin; however, it inhibited the expression of E-cadherin. In contrast, KDM5B-KD increased the expression of E-cadherin but decreased that of N-cadherin and vimentin. These results suggested that KDM5B facilitated the EMT process in PC cells.

Overexpression of miR-374b-5p inhibited the growth and metastasis of PANC-1 cells in vivo

To further evaluate the influence of miR-374b-5p on tumor growth, a tumor xenograft model of nude mice was established by transfecting PANC-1 cells with miR-374b-5p lentivirus. The subcutaneous tumor volume in the miR-374b-5p group was significantly smaller than that in the NC group (**Figure 5A**). In the lung metastasis model, HE staining showed that the number of metastasized tumors in nude mice lungs was significantly greater in the miR-374b-5p group than in the NC group (**Figure 5B**). IHC analysis revealed that KDM5B was upregulated in PC tissues compared with adjacent healthy tissues; however, miR-374b-5p expression was significantly lower in the PC tissues than in the normal tissues (**Figure 5C**). Taken together, these results indicated that miR-374b-5p inhibited PC proliferation and metastasis via KDM5B.

Discussion

Recent studies have revealed that miR-374b-5p exhibits anticancer effects in multiple cancers. For instance, miR-374b-5p suppresses the migration and invasion abilities of bladder, ovarian, and hepatocellular cancer cells [17-19]. MiR-374b-5p expression in peripheral blood can help in distinguishing prostate cancer cases from healthy controls and benign prostatic hyperplasia cases, with an AUC of 0.85 [20]. In PDAC, miR-374b-5p can ameliorate chemotherapeutic resistance by targeting several anti-apoptotic proteins [21]. However, the effect of miR-374b-5p on EMT has not yet been determined.

In the present study, miR-374b-5p was found to be downregulated in PDAC tissues; this was validated using 78 paired PDAC samples. In the PDAC cohort, it was possible to use the miR-374b-5p expression value to distinguish tumor tissues from healthy tissues. A low miR-374b-5p level was associated with more lymph node metastasis, which indicated tumor

miR-374b-5p inhibits EMT in pancreatic cancer

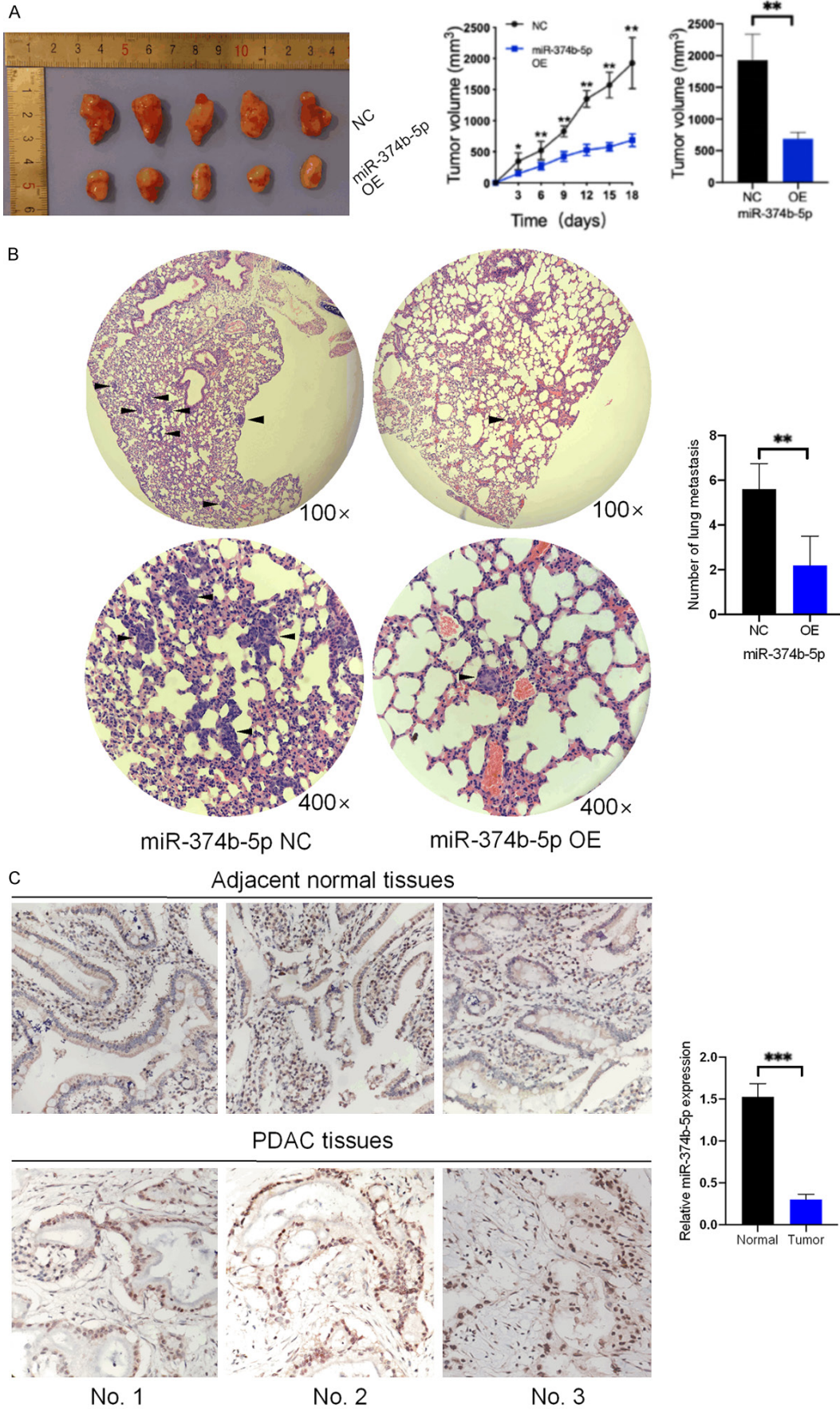


Figure 5. Overexpression of miR-374b-5p inhibited the proliferation and metastasis of PANC-1 cells *in vivo*. A. PANC-1 cells transfected with miR-374b-5p or NC were injected into nude mice subcutaneously (n = 5). After 18 days, xenograft tumors were harvested and tumor growth rate and weight were measured. B. PANC-1 cells with overexpressed miR-374b-5p or NC were injected into the tail vein of nude mice (n = 3). After 28 days, the lungs were harvested to calculate the number of metastasized tumors (100 ×). C. Immunohistochemical staining of KDM5B (200 ×) and miR-374b-5p expression in paired PDAC and adjacent normal tissues. Here are three pairs of typical photographs. Data are presented as mean ± SD. **P* < 0.05; ***P* < 0.01; ****P* < 0.001. SD, standard deviation; NC, negative control; PDAC, pancreatic ductal adenocarcinoma; OE, overexpression.

PC cells. Thus, these findings implied that miR-374b-5p functioned as a tumor suppressor for PC.

KDM5B, a histone demethylase, can remove the methylated modification at the fourth lysine of histone 3 [24] and can regulate stem cell differentiation, promote cell proliferation, inhibit gene transcription, and maintain genome stability [25]. Overexpression of KDM5B has been reported in several cancers, including prostate, breast, and gastric cancers [26-28]. A high KDM5B level is associated with poor survival and is regarded as an independent risk factor for head and neck cancer [15]. Mechanistic studies have also demonstrated that KDM5B might promote the expression of MALAT1, which in turn supports breast cancer progression [29]. In contrast, HEXIM1, a tumor-suppressive gene, is re-expressed in breast cancer cells treated with a KDM5B inhibitor [30]. Several miRNAs, including miR-424-5p [31], miR-194 [32], and miR-135b-5p [33] can bind to the 3'-UTR of KDM5B and exert anti-cancer effects. Consequently, KDM5B is a potential oncogene and a promising drug target for PC therapy.

In conclusion, We provided evidence indicating that miR-374b-5p inhibits the proliferation and migration of PC cells and that its expression has prognostic implications in PC. Mechanistically, miR-374b-5p may repress the KDM5B-mediated EMT process; therefore, miR-374b-5p and/or KDM5B could be new therapeutic targets for PC.

Acknowledgements

We thank Dr. Hua Fan, Dr. Xianliang Li, Dr. Yu Liu, and Dr. Jiantao Kou for their general support and help in providing samples. This work was supported by the Beijing Municipal Science & Technology Commission, PR China [Z181100001718164] and Capital's Funds for Health Improvement and Research, Beijing, PR China [CFH 2020-2-2036].

Disclosure of conflict of interest

None.

Address correspondence to: Qiang He and Ren Lang, Department of Hepatobiliary Surgery, Beijing Chao-Yang Hospital, Affiliated to Capital Medical University, Beijing, China. Tel: +86-13701194928; Fax: +86-010-85231503; E-mail: heqiang@bjcyh.com (QH); Tel: +86-13911757869; Fax: +86-010-85231503; E-mail: langren@bjcyh.com (RL)

References

- [1] Tsai HJ and Chang JS. Environmental risk factors of pancreatic cancer. *J Clin Med* 2019; 8: 1427.
- [2] Yan L, Raj P, Yao W and Ying H. Glucose metabolism in pancreatic cancer. *Cancers (Basel)* 2019; 11: 1460.
- [3] Gonzalez-Borja I, Viudez A, Goni S, Santamaria E, Carrasco-Garcia E, Perez-Sanz J, Hernandez-Garcia I, Sala-Elarre P, Arrazubi V, Oyaga-Iriarte E, Zarate R, Arevalo S, Sayar O, Vera R and Fernandez-Irigoyen J. Omics approaches in pancreatic adenocarcinoma. *Cancers (Basel)* 2019; 11: 1052.
- [4] McGuigan A, Kelly P, Turkington RC, Jones C, Coleman HG and McCain RS. Pancreatic cancer: a review of clinical diagnosis, epidemiology, treatment and outcomes. *World J Gastroenterol* 2018; 24: 4846-4861.
- [5] Subramani R, Gangwani L, Nandy SB, Arumugam A, Chattopadhyay M and Lakshmanaswamy R. Emerging roles of microRNAs in pancreatic cancer diagnosis, therapy and prognosis (review). *Int J Oncol* 2015; 47: 1203-1210.
- [6] Carpenter ES, Steele NG and Pasca di Magliano M. Targeting the microenvironment to overcome gemcitabine resistance in pancreatic cancer. *Cancer Res* 2020; 80: 3070-3071.
- [7] Perri G, Prakash L and Katz MHG. Defining and treating borderline resectable pancreatic cancer. *Curr Treat Options Oncol* 2020; 21: 71.
- [8] Beuran M, Negoii I, Paun S, Ion AD, Bleotu C, Negoii RI and Hostiuic S. The epithelial to mesenchymal transition in pancreatic cancer: a systematic review. *Pancreatology* 2015; 15: 217-225.
- [9] Lim LP, Lau NC, Garrett-Engle P, Grimson A, Schelter JM, Castle J, Bartel DP, Linsley PS and

miR-374b-5p inhibits EMT in pancreatic cancer

- Johnson JM. Microarray analysis shows that some microRNAs downregulate large numbers of target miRNAs. *Nature* 2005; 433: 769-773.
- [10] Zhang Z, Pan B, Lv S, Ji Z, Wu Q, Lang R, He Q and Zhao X. Integrating microRNA expression profiling studies to systematically evaluate the diagnostic value of microRNAs in pancreatic cancer and validate their prognostic significance with the cancer genome atlas data. *Cell Physiol Biochem* 2018; 49: 678-695.
- [11] Zhao F, Wei C, Cui M, Xia Q, Wang S and Zhang Y. Prognostic value of microRNAs in pancreatic cancer: a meta-analysis. *Aging (Albany NY)* 2020; 12: 9380-9404.
- [12] Chen S, Xu J, Su Y, Hua L, Feng C, Lin Z, Huang H and Li Y. MicroRNA-145 suppresses epithelial to mesenchymal transition in pancreatic cancer cells by inhibiting TGF-beta signaling pathway. *J Cancer* 2020; 11: 2716-2723.
- [13] Dai C, Zhang Y, Xu Z and Jin M. MicroRNA-122-5p inhibits cell proliferation, migration and invasion by targeting CCNG1 in pancreatic ductal adenocarcinoma. *Cancer Cell Int* 2020; 20: 98.
- [14] Tay Y, Rinn J and Pandolfi PP. The multilayered complexity of ceRNA crosstalk and competition. *Nature* 2014; 505: 344-352.
- [15] Xing C, Ye H, Wang W, Sun M, Zhang J, Zhao Z and Jiang G. Circular RNA ADAM9 facilitates the malignant behaviours of pancreatic cancer by sponging miR-217 and upregulating PRSS3 expression. *Artif Cells Nanomed Biotechnol* 2019; 47: 3920-3928.
- [16] Liu Y, Wang J, Dong L, Xia L, Zhu H, Li Z and Yu X. Long noncoding RNA HCP5 regulates pancreatic cancer gemcitabine (GEM) resistance by sponging Hsa-miR-214-3p to target HDGF. *Onco Targets Ther* 2019; 12: 8207-8216.
- [17] Wang S, Zhang G, Zheng W, Xue Q, Wei D, Zheng Y and Yuan J. MiR-454-3p and miR-374b-5p suppress migration and invasion of bladder cancer cells through targeting ZEB2. *Biosci Rep* 2018; 38: BSR20181436.
- [18] Li H, Liang J, Qin F and Zhai Y. MiR-374b-5p-FOXP1 feedback loop regulates cell migration, epithelial-mesenchymal transition and chemosensitivity in ovarian cancer. *Biochem Biophys Res Commun* 2018; 505: 554-560.
- [19] Yin Z, Ma T, Yan J, Shi N, Zhang C, Lu X, Hou B and Jian Z. LncRNA MAGI2-AS3 inhibits hepatocellular carcinoma cell proliferation and migration by targeting the miR-374b-5p/SMG1 signaling pathway. *J Cell Physiol* 2019; 234: 18825-18836.
- [20] Pang C, Song X, Fu C, Zhang Y, Zhang Y and Liu M. Diagnostic value of peripheral blood miR-374b-5p in patients with prostate cancer. *Clin Lab* 2020; 66.
- [21] Sun D, Wang X, Sui G, Chen S, Yu M and Zhang P. Downregulation of miR-374b-5p promotes chemotherapeutic resistance in pancreatic cancer by upregulating multiple anti-apoptotic proteins. *Int J Oncol* 2018; 52: 1491-1503.
- [22] Lee HS, An C, Hwang HK, Roh YH, Kang H, Jo JH, Chung MJ, Park JY, Kang CM, Park SW, Yoon DS, Lee WJ, Song SY and Bang S. Preoperative prediction of futile surgery in patients with radiologically resectable or borderline resectable pancreatic adenocarcinoma. *J Gastroenterol Hepatol* 2020; 35: 499-507.
- [23] Shen YN, Bai XL, Jin G, Zhang Q, Lu JH, Qin RY, Yu RS, Pan Y, Chen Y, Sun PW, Guo CX, Li X, Ma T, Li GG, Gao SL, Lou JY, Que RS, Lau WY and Liang TB. A preoperative nomogram predicts prognosis of up front resectable patients with pancreatic head cancer and suspected venous invasion. *HPB (Oxford)* 2018; 20: 1034-1043.
- [24] Seward DJ, Cubberley G, Kim S, Schonewald M, Zhang L, Tripet B and Bentley DL. Demethylation of trimethylated histone H3 Lys4 in vivo by JARID1 JmjC proteins. *Nat Struct Mol Biol* 2007; 14: 240-242.
- [25] Li X, Liu L, Yang S, Song N, Zhou X, Gao J, Yu N, Shan L, Wang Q, Liang J, Xuan C, Wang Y, Shang Y and Shi L. Histone demethylase KDM5B is a key regulator of genome stability. *Proc Natl Acad Sci U S A* 2014; 111: 7096-7101.
- [26] Xiang Y, Zhu Z, Han G, Ye X, Xu B, Peng Z, Ma Y, Yu Y, Lin H, Chen PA and Chen CD. JARIDIB is a histone H3 lysine 4 demethylase up-regulated in prostate cancer. *Proc Natl Acad Sci U S A* 2007; 104: 19226-19231.
- [27] Ilic M and Ilic I. Epidemiology of pancreatic cancer. *World J Gastroenterol* 2016; 22: 9694-9705.
- [28] Wang Z, Tang F, Qi G, Yuan S, Zhang G, Tang B and He S. KDM5B is overexpressed in gastric cancer and is required for gastric cancer cell proliferation and metastasis. *Am J Cancer Res* 2014; 5: 87-100.
- [29] Bamodu OA, Huang WC, Lee WH, Wu A, Wang LS, Hsiao M, Yeh CT and Chao TY. Aberrant KDM5B expression promotes aggressive breast cancer through MALAT1 overexpression and downregulation of hsa-miR-448. *BMC Cancer* 2016; 16: 160.
- [30] Montano MM, Yeh IJ, Chen Y, Hernandez C, Kiselar JG, de la Fuente M, Lawes AM, Nieman MT, Kiser PD, Jacobberger J, Exner AA and Lawes MC. Inhibition of the histone demethylase, KDM5B, directly induces re-expression of tumor suppressor protein HEXIM1 in cancer cells. *Breast Cancer Res* 2019; 21: 138.
- [31] Zakaria HM, Mohamed A, Omar H and Gaballa NK. Alpha-fetoprotein level to total tumor volume as a predictor of hepatocellular carcinoma recurrence after resection. A retrospective

miR-374b-5p inhibits EMT in pancreatic cancer

- cohort study. *Ann Med Surg (Lond)* 2020; 54: 109-113.
- [32] Bao J, Zou J, Li C and Zheng G. miR-194 inhibits gastric cancer cell proliferation and tumorigenesis by targeting KDM5B. *Eur Rev Med Pharmacol Sci* 2016; 20: 4487-4493.
- [33] Ren R, Wu J and Zhou M. MiR-135b-5p affected malignant behaviors of ovarian cancer cells by targeting KDM5B. *Eur Rev Med Pharmacol Sci* 2020; 24: 3548-3554.